

An Experimental Investigation of Low Power, Long Duration Rotamak Discharges

I. R. Jones,^{A,C} M. D. E. Turley,^A J. E. Wedding,^A G. Durance,^B
G. R. Hogg^B and J. Tendys^B

^A School of Physical Sciences, Flinders University of South Australia,
Bedford Park, S.A. 5042.

^B Australian Atomic Energy Commission Research Establishment,
Lucas Heights Research Laboratories, Private Mail Bag, Sutherland, N.S.W. 2232.

^C AAEC Senior Consultant (Fusion Physics).

Abstract

A rotamak device is described in which compact torus plasmas are generated using relatively low RF input powers (\sim a few kW). Compact torus configurations are generated in both argon and hydrogen plasmas and are sustained for ~ 9 ms. These configurations appear to be grossly stable and show no tendency to disrupt even when subjected to large amplitude forced oscillations. A configuration incorporating a toroidal field is also investigated.

1. Introduction

The technique of driving an electron current by means of a rotating magnetic field of appropriate amplitude and angular frequency is well established (Blevin and Thonemann 1962; Hugrass *et al.* 1981). The application of this technique for the express purpose of generating and maintaining a compact torus configuration has given rise to a concept known as the rotamak (Jones 1979; Hugrass *et al.* 1980). The rotamak is a compact torus device in which a rotating magnetic field is used to generate and maintain the toroidal plasma current. Equilibrium requires the presence of an additional poloidal field (the 'vertical field' of tokamak research) which couples with the toroidal current to produce the necessary inward force.

The initial rotamak experiments used high power, short duration (\sim few MW, ~ 100 μ s) RF pulses and convincingly demonstrated that the desired compact torus configurations could be achieved (Hugrass *et al.* 1980; Durance *et al.* 1982; Durance and Jones 1986). However, the duration of these experiments was too short to unambiguously demonstrate that the resulting configurations were grossly stable. Experiments have now been completed at both Flinders University and the Australian Atomic Energy Commission with RF pulses of longer duration but much lower power (\sim few kW, ~ 20 ms). Despite the low RF power, compact torus configurations have been generated and sustained for the full duration of the RF pulses. These are the longest-lived compact torus configurations achieved by any method to date. The purpose of this paper is to present some of the more interesting experimental observations made in these low power studies.

2. Experimental Apparatus

Although there were differences in the equipment used at Flinders University and the AAEC, the devices were sufficiently similar for a generalised description to suffice.

A schematic diagram of the experimental apparatus is shown in Fig. 1. The rotating magnetic field was generated by feeding two RF current pulses (dephased by 90°) into a pair of orthogonal Helmholtz coils mounted on the outside of a spherical pyrex glass discharge vessel (0.28 m in diameter). The RF current pulses were generated with an oscillator (0.8 MHz, 6 kW) at Flinders University and with an RF source/linear amplifier system (1.0 MHz, 6 kW) at the AAEC. In both cases, the duration of the RF pulses was limited to ≤ 20 ms to avoid problems with components overheating. Impedance matching circuits were used to couple the oscillator/amplifier outputs to the Helmholtz coils. In principle, it is possible to tune the matching circuits to maximise the power transferred to the plasma for any type of plasma discharge (i.e. for any arbitrary set of initial conditions of gas filling pressure and externally applied equilibrium field amplitude). However, in practice, the matching circuits were only adjusted for one given set of initial conditions and further fine tuning was not attempted.

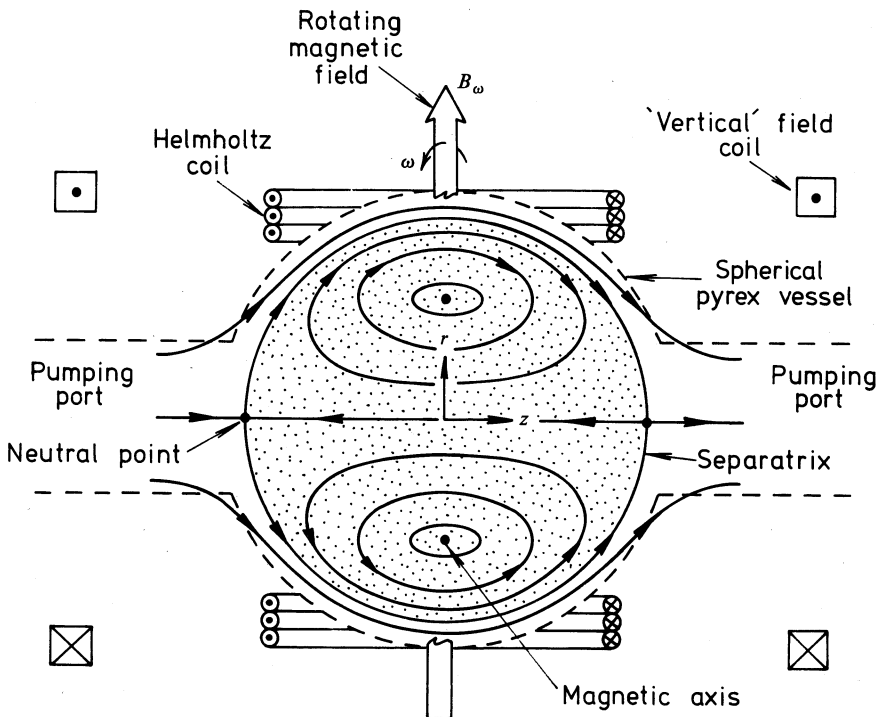


Fig. 1. Schematic diagram of the rotamak apparatus.

The externally imposed magnetic field required for plasma equilibrium was produced by two coils of mean diameter 0.3 m positioned symmetrically about the discharge vessel with a coil separation of 0.5 m. The rise time, amplitude and duration of the current waveforms supplied to these coils were all adjustable. Throughout this paper,

this imposed equilibrium field will be characterised by its amplitude at the centre of the discharge vessel in the absence of plasma.

A turbomolecular pump maintained the base pressure of the vacuum system at $\sim 1 \times 10^{-6}$ Torr (1 Torr \equiv 133 Pa). During operation, the filling gas was continuously bled through the system via a piezo-electric valve. The filling pressure was monitored with an ionisation gauge. The pressures quoted in this paper have been corrected for the gauge sensitivity.

The filling gas was weakly pre-ionised by passing a ~ 20 MHz current pulse through two six-turn coils wound on each pumping arm. The duration of this current pulse was limited to ~ 1 s prior to the main RF discharge and overlapped the main discharge by ~ 1 ms.

The discharge vessel was equipped with a Rogowski coil threaded through a central axial glass tube and around the outer surface of the vessel so as to enclose a complete minor cross section of the plasma torus. This coil measured the total toroidal plasma current driven by the rotating field.

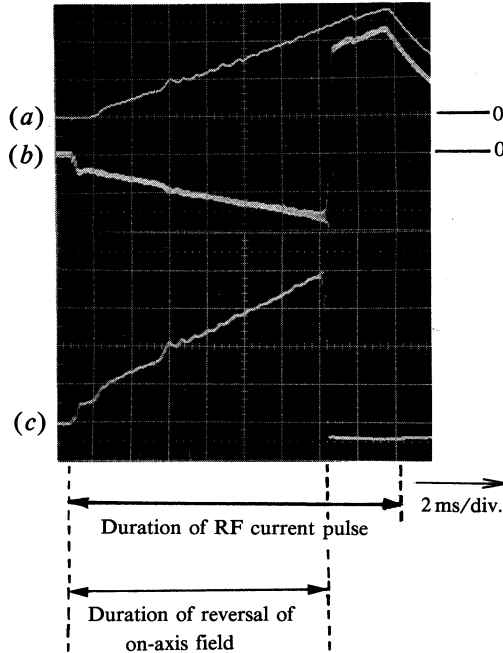


Fig. 2. (a) Waveform of the applied equilibrium field as measured in vacuo at $r = 1$ cm and $z = 0$ (7.2 G/div.). (b) The z component of the resultant magnetic field at $r = 1$ cm and $z = 0$ during a plasma discharge (6.6 G/div.). (c) The driven plasma current I_ϕ (131 A/div.).

An axial glass tube (~ 6 mm o.d.) provided access for magnetic probes, while radial access was provided in the equatorial toroidal plane by two ports equipped with retractable glass probe guides (~ 5.6 mm o.d.). Both Hall-effect probes and miniature wire-wound probes were used to measure the various magnetic field components.

Voltage and current probes were used to determine the RF power transferred to the plasma. Also, an 8 mm microwave interferometer was used to measure the line-averaged electron number density.

3. Experimental Results

(a) *Some General Observations*

The application of the rotating field to the pre-ionised plasma drives toroidal plasma current which reverses the externally applied equilibrium field and generates a compact torus configuration. Normally, the discharge is observed to terminate when either the RF current pulse or the externally applied equilibrium field terminates. The magnitude of the driven toroidal plasma current is observed to be approximately proportional to the amplitude of the applied equilibrium field in a manner similar to that observed in the earlier short duration, high power experiments (Durance and Jones 1986). Thus the amplitude of the driven current can be increased simply by increasing the amplitude of the applied equilibrium field. There is, however, an upper limit to the amount of toroidal current which can be driven. Endeavouring to exceed this limit by further increasing the amplitude of the equilibrium field results in the discharge terminating, even though the rotating field and the equilibrium field are still being applied. This behaviour is illustrated in Fig. 2 where a 'ramped' equilibrium field is applied (see Fig. 2*a*) and the resulting driven toroidal plasma current, $I_{\phi}(t)$, increases with time, following the general shape of the equilibrium field, until it reaches a value of ~ 560 A, whereupon it terminates suddenly (see Fig. 2*c*). The z component of the field near the central axis, $B_z(r=1 \text{ cm}, z=0, t)$, is used as an indicator of the time for which a compact torus configuration is generated (i.e. the time for which the on-axis field is reversed; see Fig. 2*b*).

Similar results were obtained for other rise-time/amplitude combinations of the applied equilibrium field. The driven plasma current always terminated when it reached a critical value of 560 ± 15 A; the corresponding value of the applied equilibrium field was 15.8 ± 0.3 G ($1 \text{ G} \equiv 10^{-4} \text{ T}$). If the applied equilibrium field did not exceed this critical value, the discharge proceeded until either the RF or the equilibrium field terminated.

It is believed that a normal rotamak discharge can only exist if the constraints of both pressure balance and power balance are simultaneously satisfied. It is therefore surmised that the termination shown in Fig. 2 arises from the inability of the RF supply to furnish the power which is associated with the generation of toroidal currents greater than ~ 560 A in the present plasmas. (This includes the power dissipated by the RF screening currents which will inevitably be present to some extent.)

For any given equilibrium field amplitude, the driven toroidal current was observed to have a slight dependence on the initial gas filling pressure: the current increased as the gas filling pressure was reduced. However, if the filling pressure was too low, the discharge failed to strike. For the experiments reported here, the filling pressures were in the range ~ 0.3 – 1.0 mTorr.

For any given combination of gas filling pressure and applied equilibrium field amplitude, the discharge characteristics were found to be highly reproducible and the discharge was observed to be grossly stable.

These general observations apply to both argon and hydrogen discharges.

(b) Rotamak Discharges in Argon

In this subsection we present the results of detailed measurements made on one particular argon rotamak discharge having as initial conditions a filling pressure of 0.35 mTorr and an externally applied equilibrium magnetic field of the waveform shown in Fig. 3a (i.e. a 'flat-top' equilibrium field case). The steady state amplitude of the applied equilibrium field at the centre of the discharge vessel was 12.5 G in this case. The envelope of one of the RF current pulses used to generate the applied rotating magnetic field is shown in Fig. 3b. The 300 Hz amplitude (and hence power) modulation seen on this pulse is caused by a modulation in the plate supply of the RF power source; its presence is evident on most experimentally measured parameters.

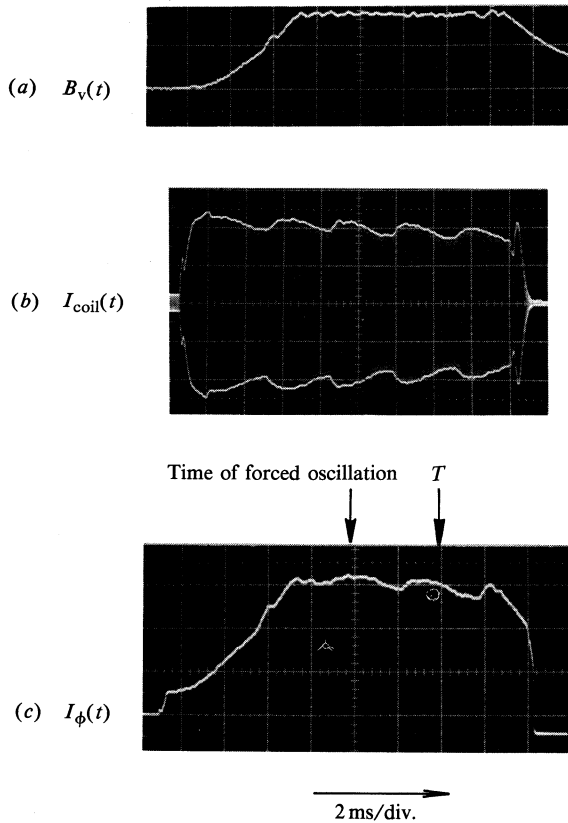


Fig. 3. (a) Waveform of the applied equilibrium field as measured at $r = 1$ cm and $z = 0$ (7.2 G/div.). (b) Envelope of the RF current pulse through one of the Helmholtz coils (14.5 A/div.). (c) The driven plasma current I_ϕ (131 A/div.).

Driven Toroidal Current $I_\phi(t)$

An oscillogram of the total toroidal current driven by the rotating magnetic field in this particular rotamak discharge is shown in Fig. 3c. After an initial rise in the current which mirrors the rise in the applied vertical field, the driven current is seen

to be maintained at a substantially constant value of ~ 400 A for the duration of the rotating field pulse.

Magnetic Field and Flux Measurements

The magnetic field in a rotamak discharge has a quasi-steady (d.c.) poloidal component which is a combination of the externally imposed equilibrium field and the poloidal field generated by the driven toroidal current. Its components are $B_r(r, z)$ and $B_z(r, z)$. The magnetic field has also oscillating (RF) components, $B_r(r, \phi, z, t)$ and $B_\phi(r, \phi, z, t)$, which are associated with the applied rotating field. If the penetration of the rotating field into the plasma is only partial there will be, in addition, oscillating components which are due to RF screening currents in the plasma.

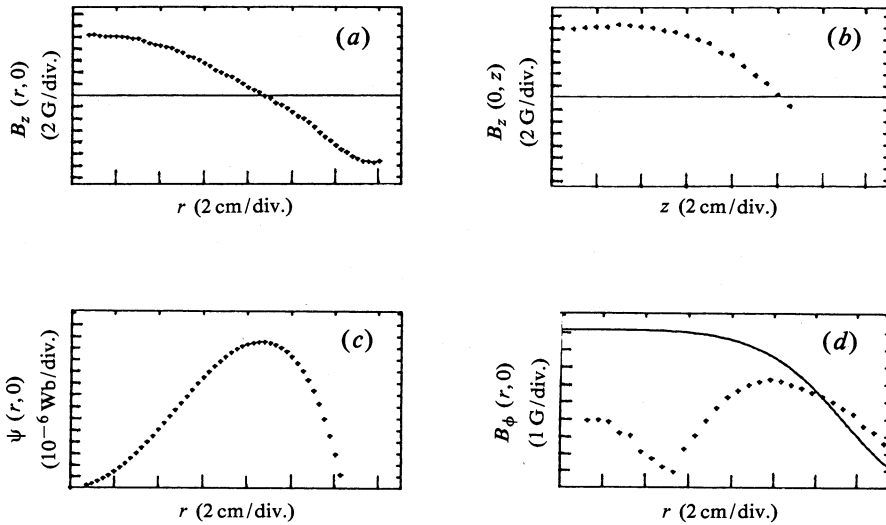


Fig. 4. Results of magnetic probe measurements made at time T shown in Fig. 3: (a) radial distribution of the z component of the magnetic field in the equatorial plane; (b) axial distribution of the z component of the magnetic field for $r = 0$; (c) the poloidal flux function calculated from (a); and (d) penetration of the rotating magnetic field into the plasma (dotted curve, measured; solid curve, calculated assuming complete penetration).

Quasi-steady (d.c.) poloidal magnetic field. The B_z component of the quasi-steady poloidal field was measured as a function of time at 54 points (2.5 mm apart) along the r axis in the $z = 0$ plane. This enabled the radial profiles of $B_z(r, 0)$ to be constructed at selected times throughout the rotamak discharge. Fig. 4a shows one such profile corresponding to the time T , identified in Fig. 3. Since each experimental point in Fig. 4a arises from a different experimental discharge, the smoothness of the data testifies to the high degree of reproducibility which is achieved in rotamak discharges. The position of the magnetic axis [i.e. where $B_z(r, 0) = 0$] is readily identified from such profiles. Fig. 4c shows the results of numerically integrating the $B_z(r, 0)$ data to obtain the radial distribution of the poloidal flux function

$$\psi(r, 0) = 2\pi \int_0^r r' B_z(r', 0) dr'.$$

The radial position of the separatrix in the $z = 0$ plane is easily determined [i.e. where $\psi(r, 0) = 0$].

The z component of the quasi-steady poloidal field was measured at 22 points (5 mm apart) along the z axis. The axial profile at the time T is shown in Fig. 4*b*. The position of the neutral point [i.e. where $B_z(0, z) = 0$] is clearly evident.

From an analysis of several consecutive profiles of the type shown in Figs 4*a*–4*c*, the trajectories of the separatrix at $x = 0$ (R_s), the magnetic axis (r_m) and the neutral point (Z_x) could be obtained; these are shown in Fig. 5*a*. After an initial contraction, the magnetic configuration settles down to an equilibrium state for which $R_s/r_m = 1.42$ and $R_s/Z_x = 1.23$. The configuration is that of an oblate compact torus having its separatrix surface lying entirely within the discharge vessel. It is maintained in an apparently stable steady state for ~ 9 ms; its termination coincides with the end of the rotating field pulse.

Oscillating (RF) magnetic field component. A uniform magnetic field, rotating about the z axis with an angular frequency ω , can be described in cylindrical coordinates (r, ϕ, z) by the equations

$$B_r = B_\omega \cos(\omega t - \phi), \quad B_\phi = B_\omega \sin(\omega t - \phi),$$

where B_ω is the amplitude of the rotating field. In this experiment the envelope of the time derivative of the ϕ component, i.e. $\partial B_\phi / \partial t$, was recorded and, assuming that this was proportional to the envelope of B_ϕ , was used as a measure of penetration of the externally imposed rotating magnetic field into the plasma. To quantify the degree of field penetration, the measured radial profile of the amplitude of the B_ϕ signal was compared with that corresponding to complete penetration. This latter quantity was computed from a knowledge of the rotating field coil geometry and the RF currents passing through them.

The measured radial distribution of B_ϕ at time T is shown in Fig. 4*d*; the computed profile corresponding to complete penetration is shown as the solid curve. The rotating field fails to completely penetrate the interior of the plasma. Nevertheless, the mere observation of driven toroidal plasma current allows us to assert that the penetration is better than that to be expected on the basis of the classical skin effect (Jones and Hugrass 1981).

Electron Density Measurement

The average electron number density $\bar{n}_e(t)$ along a chord of the plasma was measured using an 8 mm microwave interferometer. It was assumed that the electrons resided within the separatrix at all times and the appropriate chord length was calculated using the measured values of R_s and Z_x . The particular chord used in this experiment was one which passed right through the compact torus configuration just below the $z = 0$ plane. The corresponding time history of $\bar{n}_e(t)$ is shown in Fig. 5*b*.

In Fig. 5*a* an early contraction of the magnetic configuration is clearly identifiable. Fig. 5*b* shows that an increase in \bar{n}_e is associated with this contraction. It is observed that, to within experimental error, the total number of electrons is conserved during this contraction and subsequent expansion. Thereafter, during the ~ 9 ms of steady state, \bar{n}_e decays at a slow rate.

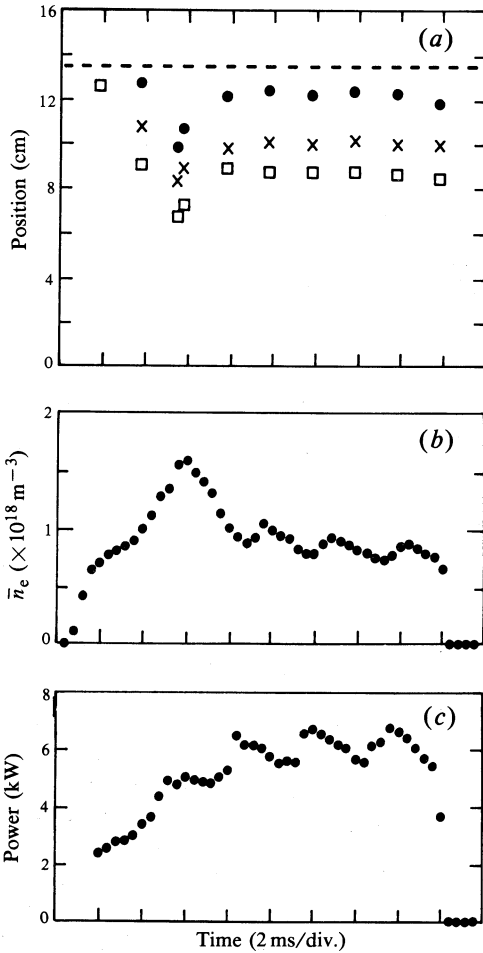


Fig. 5. (a) Position of the separatrix R_s (circles), neutral point Z_x (crosses) and the magnetic axis r_m (squares) as a function of time during the argon discharge.

(b) Time dependence of the average electron density.

(c) Measured RF power input into the plasma as a function of time.

RF Input Power Measurement

The driving of toroidal plasma current in the rotamak discharge requires a transfer of power from the RF source to the plasma. By measuring the appropriate RF currents and voltages and the phases between them and by making due allowance for the fixed losses in the matching circuits, it is possible to calculate the average RF power dissipated in the plasma. This quantity is shown as a function of time in Fig. 5c. About 6 kW of RF power is required to maintain this particular rotamak discharge in steady state.

Forced Radial Oscillation of the Rotamak Equilibrium

A preliminary experimental investigation of the forced oscillation of the rotamak configuration has been undertaken with a view to possible diagnostic and, in the longer term, heating applications. The response of the steady state argon rotamak equilibrium described above to forced oscillations was investigated by superimposing an oscillation on the externally applied equilibrium field by means of auxiliary coils. This was done during the short time interval ($\sim 200 \mu\text{s}$) indicated in Fig. 3c.

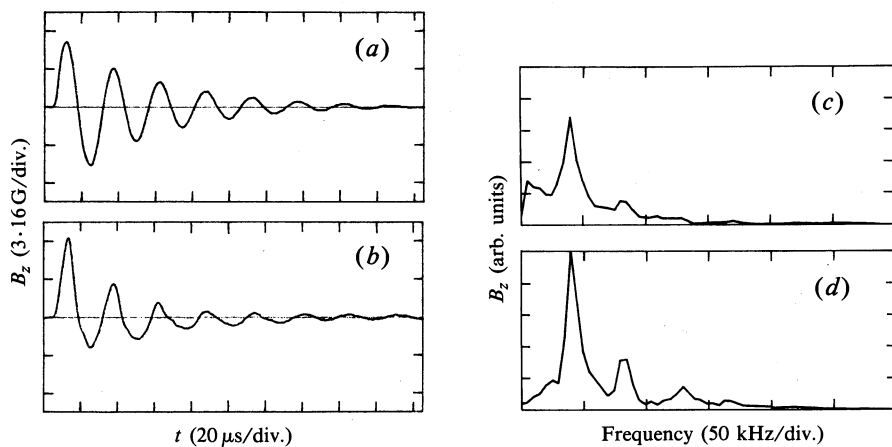


Fig. 6. (a) The z component of the superimposed oscillatory magnetic field as measured in vacuo at $r = 1.5$ cm and $z = 0$. (b) The z component of the oscillatory magnetic field measured during a plasma discharge at $r = 10.5$ cm and $z = 0$. (c) Frequency spectrum of the z component of the oscillatory magnetic field measured during a plasma discharge at $r = 10.5$ cm and $z = 0$. (d) Frequency spectrum of the z component of the oscillatory magnetic field measured during a plasma discharge at $r = 0$ and $z = 8.0$ cm.

Initially, the response to a short duration (~ 3 μ s) impulse superimposed on the equilibrium field was investigated. Fourier analysis of the magnetic probe signals indicated that the magnetic field structure of the rotamak responded with an oscillatory motion of frequency ~ 40 kHz. Resonant excitation of the magnetic configuration at this frequency was then attempted by superimposing on the equilibrium field a damped oscillatory component (40.1 kHz) generated by a conventional capacitor discharge. The z component of this superimposed oscillatory magnetic field, measured at $r = 1.5$ cm in the $z = 0$ plane in the absence of plasma, is shown in Fig. 6a. The frequency spectrum of this signal shows only a peak at the fundamental frequency; there is no evidence of components at the second and higher harmonics. The perturbation is not small; its peak value of $\lesssim 5$ G is to be compared with the 12.5 G of the applied equilibrium field.

The z component of the oscillatory magnetic field was measured at 27 radial positions under discharge conditions. The signal at one representative radial position is shown in Fig. 6b. Fourier analysis of this data shows a strong component at the fundamental frequency with some response at the second harmonic and a smaller response at the third harmonic (see Fig. 6c).

From the measured B_z data and from a knowledge of the underlying equilibrium, it is possible to construct the radial distribution of the z component of the *total* poloidal magnetic field in the $z = 0$ plane at any given instant of time, and hence the corresponding radial profile of the flux function ψ . Such constructions were made for a number of consecutive times, each being separated from the next by one-eighth the period of the excitation. A set of poloidal flux functions corresponding to one complete period of the forced oscillation is shown in Fig. 7a. The solid curves in Fig. 7a show the flux function corresponding to the underlying equilibrium. A radial movement of the maximum of the flux function is seen in Fig. 7a. The maximum

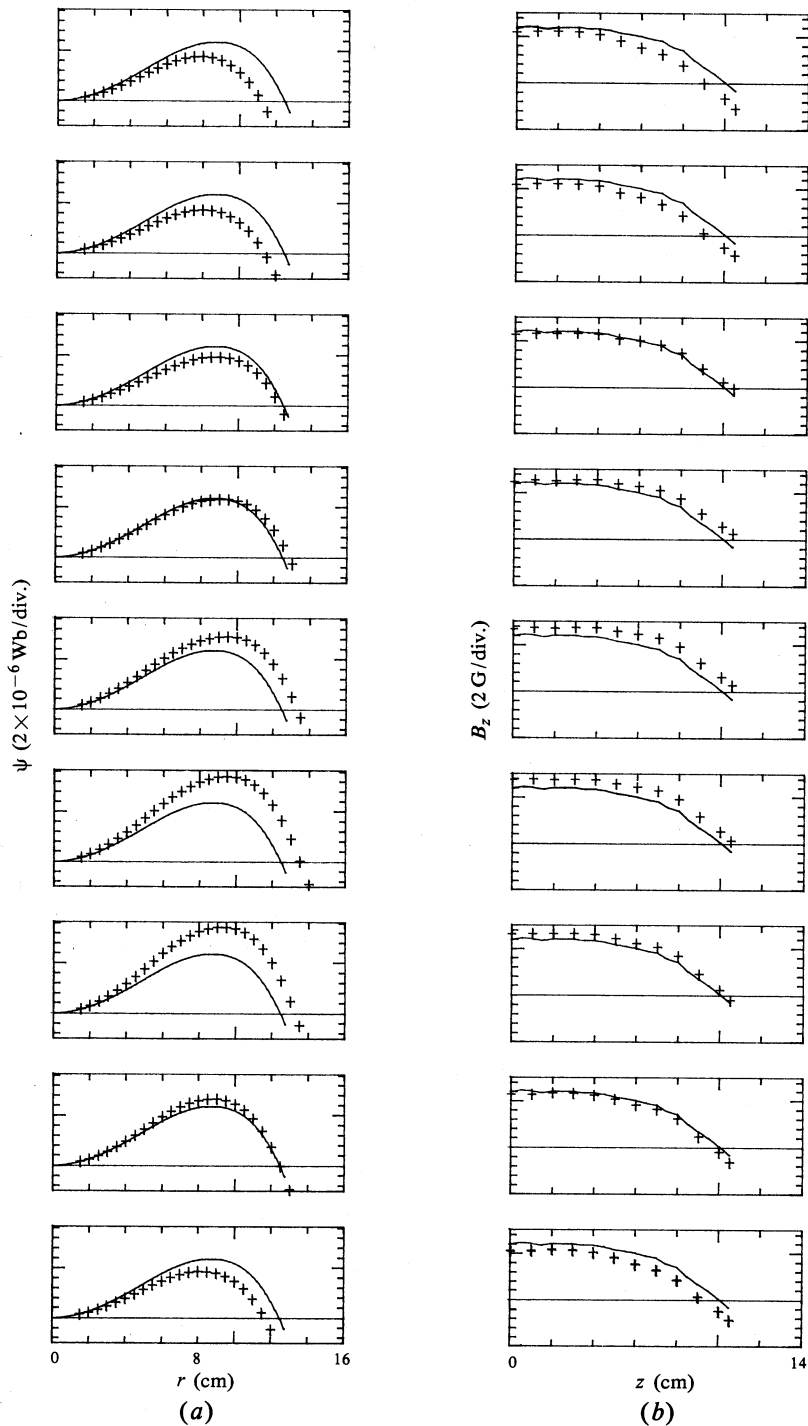


Fig. 7. (a) Radial distribution of the poloidal flux function in the equatorial plane as measured at a series of time steps, spaced $1/8$ period apart, during a plasma discharge. Solid curves represent the flux function corresponding to the underlying equilibrium. (b) Measured axial distributions of the z component of the total poloidal magnetic field, corresponding to the same time steps as the data shown in (a), compared with the equilibrium distributions (solid curves).

value changes during a cycle, being smaller than the equilibrium value on the inward excursions and larger on the outward.

Measurements were made of the z component of the oscillating magnetic field at 12 positions along the z axis. Fourier analysis of this data showed a significantly higher second and third harmonic content than was the case for the radial data shown in Fig. 6c (see Fig. 6d). Again, these data, together with a knowledge of the underlying equilibrium, have made it possible to construct the distribution of the z component of the *total* poloidal magnetic field along the z axis at any given time. The z profiles of $B_z(0, z)$, which correspond to the same times as the radial data, are shown in Fig. 7b; the distributions corresponding to the equilibrium (solid curves) are also shown for comparison.

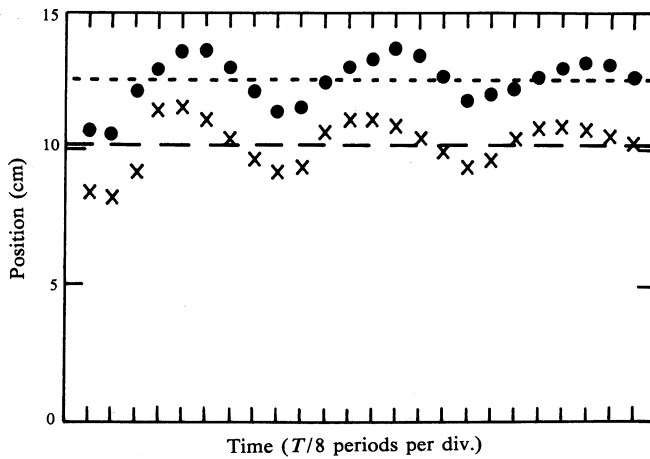


Fig. 8. Time dependence of the position of the separatrix in the equatorial plane and the position of the neutral point along the z axis compared with their positions in the underlying equilibrium: circles, separatrix position; crosses, neutral point position; dotted line, equilibrium position of separatrix; and dashed line, equilibrium position of neutral point.

The positions of the separatrix (on the $z = 0$ plane) and the neutral point were obtained as a function of time from additional data similar to that presented in Figs 7a and 7b respectively. These positions are plotted and compared with the equilibrium positions in Fig. 8. Although the data are not entirely unambiguous (due in part to some distortion of the axial B_z signal by the second harmonic), it would appear that the plasma is expanding and contracting as a whole in a 'breathing-like' mode of oscillation. Perhaps the most important observation is that this forced, large amplitude oscillatory motion does not destroy the equilibrium configuration. The rotamak discharge seems to be a robust plasma/field configuration.

(c) Rotamak Discharges in Hydrogen

Current drive by means of a rotating field is more efficient the lower the value of the electron-ion momentum transfer collision frequency ν_{ei} . In turn, ν_{ei} is proportional to n_e and it is advantageous to use low gas filling pressures. In the high power, short duration experiments (Hugrass *et al.* 1980; Durance and Jones 1986) the duration of

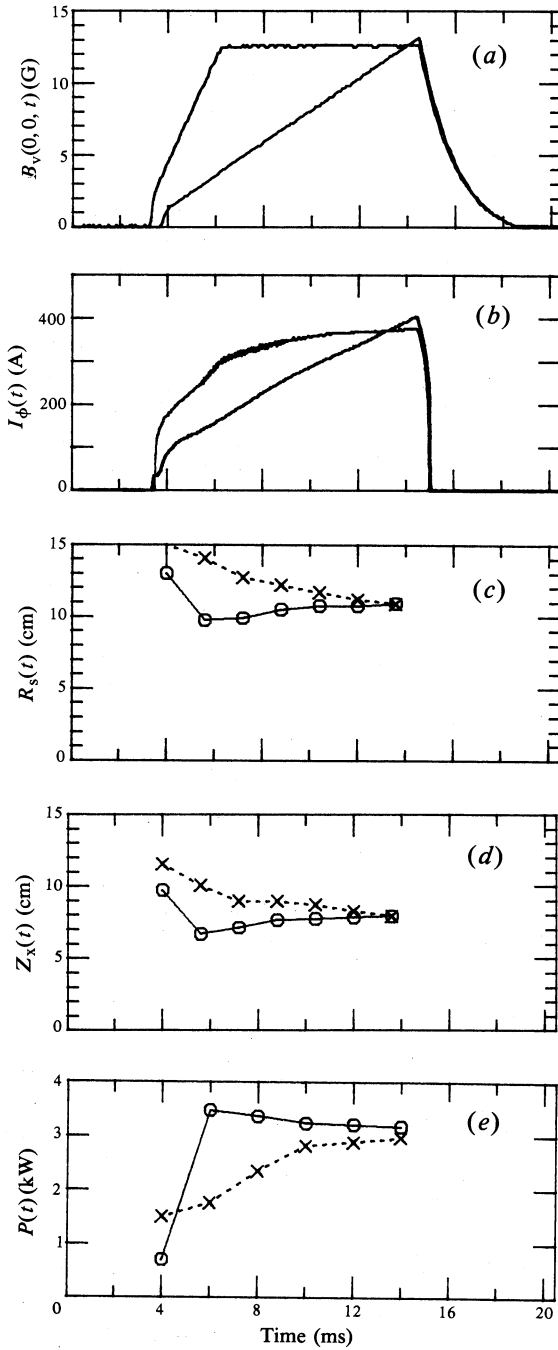


Fig. 9. Comparison of two hydrogen plasma discharges with a ramped and flat-top applied equilibrium field: (a) waveforms of the applied equilibrium fields as measured in vacuo; (b) driven toroidal currents; (c) radial position of separatrix in the equatorial plane; (d) axial positions of neutral points; (e) RF input power with crosses and circles for the ramped and flat-top equilibrium fields respectively. The wall of the discharge vessel is at $r \approx 14$ cm.

the rotating field pulse was too short to enable significant ionisation of a low pressure fill of hydrogen to occur and, consequently, low pressure fills of argon (for which ionisation proceeds at a faster rate) were used instead. In the much longer duration experiments described here, however, the slower ionisation rate of hydrogen could be accommodated and rotamak discharges using that gas could be studied.

In this subsection we report on two studies involving hydrogen discharges in which: the evolution, by quite different paths, of two normal rotamak discharges to a common equilibrium state is documented; and the influence of an externally imposed steady toroidal magnetic field is investigated.

Evolution of Rotamak Discharges

The evolution of two hydrogen rotamak discharges in response to applied equilibrium fields of quite different waveforms, but which terminate at the same amplitude, is shown in Fig. 9. The same filling pressure of 0.98 mTorr hydrogen was used in both discharges and the waveforms of the applied equilibrium field are shown in Fig. 9a. (We will refer to these two cases as 'flat top' and 'ramped'.) The driven currents $I_{\phi}(t)$, the trajectories of the separatrices and neutral points, and the RF input power corresponding to these two cases are shown respectively in Figs 9b–9e.

We note that each rotamak discharge reaches a common equilibrium state for which $I_{\phi} = 400$ A, $R_s/Z_x = 1.38$ (oblate) and the RF power input to the plasma is 3 kW. Each discharge, however, reaches this final state by a different path. The driven currents are observed to follow approximately the waveform of the corresponding applied equilibrium fields. However, in the flat-top case, the applied field rises more rapidly than the corresponding driven current as is evident, for example, by comparing the applied fields in Fig. 9b at the times when the respective driven currents have reached 300 A. Since the position of the separatrix reflects a balance between the tendency of the driven current ring to expand and the confining effect of the applied field, it is not surprising that the separatrix is observed to be at a smaller radius in the flat-top case at this time (see Fig. 9c). It is also not surprising to observe that the RF input power is closely related to the driven plasma current since this power is that which is required to sustain the driven current against ohmic dissipation.

In summary, we view the evolution of a normal rotamak discharge in response to the application of a vertical field of a predetermined waveform which varies on the millisecond timescale, as a progression through a sequence of quasi-steady equilibria. At any instant in the discharge, the existence of an equilibrium configuration demands that pressure balance prevails and that an RF power input consistent with the requirements of this equilibrium be available.

Influence of an Externally Imposed Steady Toroidal Magnetic Field

Nearly all of the rotamak research undertaken to date has been concerned with configurations having no initially imposed steady toroidal magnetic field. The working philosophy has been that, as long as the basic rotamak configuration continued to appear macroscopically stable, no additional toroidal field would be incorporated. The resulting magnetic field configuration is thus closely related to that of the field-reversed configuration although, in the rotamak case, an additional rotating magnetic field is present. Even though the inclusion of a toroidal field appears to be unnecessary from the stability point of view, the inclusion of such a field may offer other benefits such as improved particle and energy confinement.

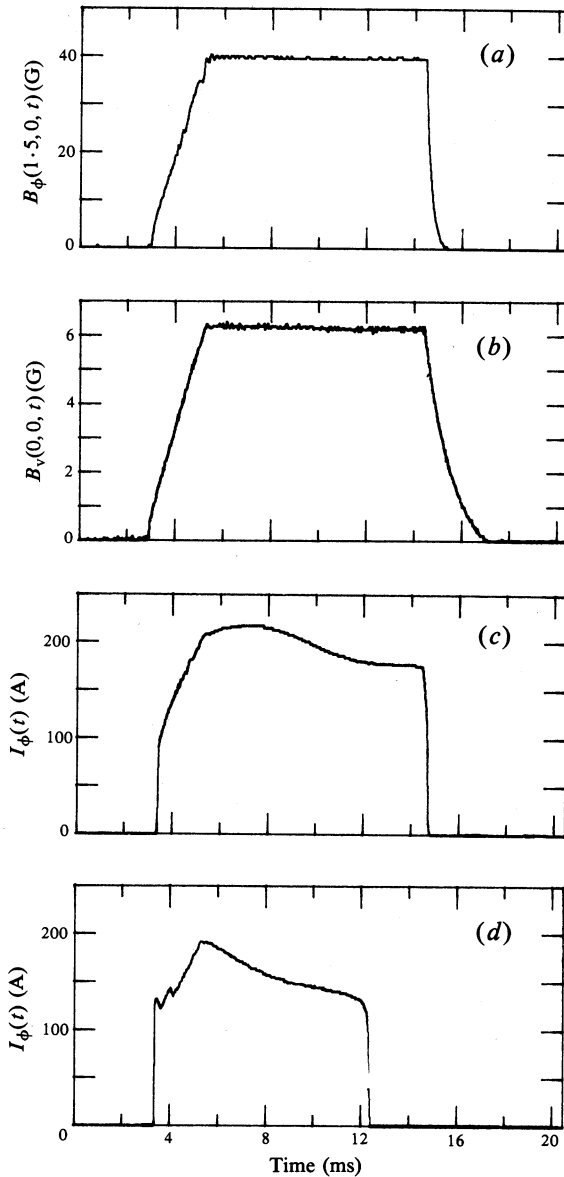


Fig. 10. (a) Waveform of the applied toroidal magnetic field measured in vacuo at $r = 1.5$ cm and $z = 0$. (b) Waveform of the applied equilibrium magnetic field measured in vacuo at $r = z = 0$. (c) Driven toroidal plasma current without the applied toroidal field. (d) Driven toroidal plasma current with the applied toroidal field.

Hugrass *et al.* (1980) performed a preliminary investigation into the effects of a toroidal magnetic field in the early high power, short duration rotamak experiments using argon as the filling gas. It was observed that the toroidal field was increased above its vacuum value by a paramagnetic poloidal current flowing in the plasma. The position of the magnetic axis was also displaced to a smaller radial position in comparison with the case of no toroidal field, consistent with toroidal equilibrium requirements.

Mention should also be made of a subsequent high power, short duration ($\sim 80 \mu\text{s}$) rotamak experiment (without an initially applied toroidal field) in which a spontaneously generated toroidal field was observed under certain conditions (Durance and Jones 1986). This field was found to be of opposite sense in the two halves of the minor cross section (i.e. the total toroidal flux was always zero). A possible explanation for the self-generation of this field has been advanced by Hugrass and Kirolous (1984). Since the appearance of this spontaneously generated field was accompanied by an increase in the driven toroidal current, it was surmised that the presence of the field aided energy confinement.

In the present experiments, the applied toroidal field was produced in the standard rotamak apparatus by passing a current ($\sim 400 \text{ A}$) through a metal rod (3.0 mm diameter) located along the z axis. The return path was via four straight conductors arranged symmetrically about and at a distance of 5 cm from the outside of the spherical discharge vessel. The rise time and duration of the current pulses to the toroidal and equilibrium magnetic field coils were identical, but the current amplitudes could be varied independently.

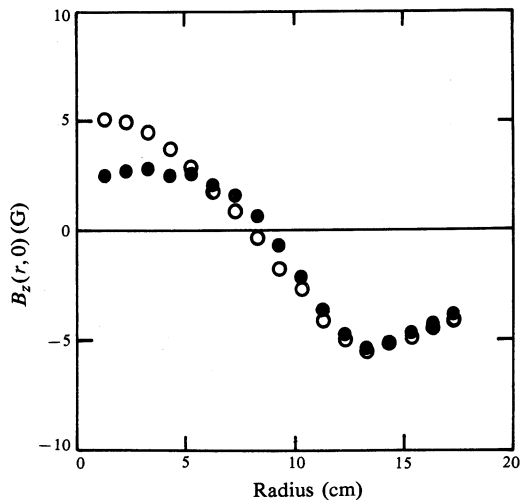


Fig. 11. Radial distribution of the z component of the poloidal field at time $t = 10 \text{ ms}$ during the discharge, both with (solid circles) and without (open circles) the applied toroidal field.

A detailed investigation was made of a rotamak discharge for which the applied toroidal field (at $r \sim 1.5 \text{ cm}$ and $z = 0$) and vertical field (at $r = z = 0$) had the waveforms shown in Figs 10a and 10b. The hydrogen filling pressure was $\sim 1.2 \text{ mTorr}$. Figs 10c and 10d show the driven toroidal current both with and without the toroidal field present. With the toroidal field present, the driven current is observed to terminate abruptly prior to the termination of either the rotating magnetic field or the applied vertical field.

Fig. 11 shows the radial distribution of the z component of the poloidal field during the discharge at time $t = 10 \text{ ms}$ for the two cases. Integration of these radial profiles enabled the radial position of the separatrix to be determined (see Fig. 12).

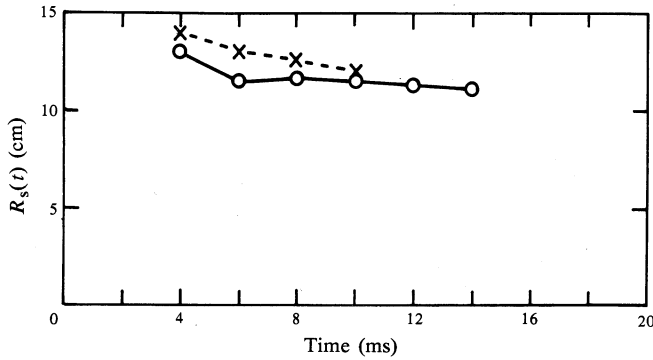


Fig. 12. Radial position of the separatrix in the equatorial plane, both with (crosses) and without (circles) the applied toroidal field.

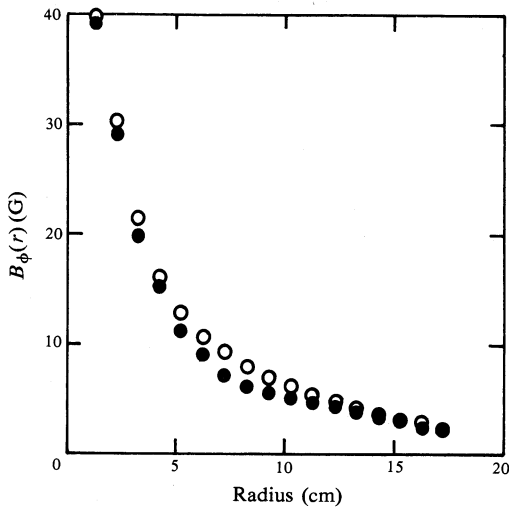


Fig. 13. Radial distribution of the toroidal magnetic field in vacuo (open circles) and during a plasma discharge (solid circles).

It is observed that the magnetic axis and the separatrix are displaced to larger radial positions when the toroidal field is applied.

The radial distributions of the toroidal field in the $z = 0$ plane, both in vacuo and during a plasma discharge, are shown in Fig. 13. The observed decrease in the toroidal field during the rotamak discharge implies that a diamagnetic current (calculated to be ~ 75 A) is generated within the plasma. This amount of poloidal current is significant when compared with the 150 A of driven toroidal current. The generation of this diamagnetic poloidal current and the shift in r_m and R_s contrast with the results obtained in the earlier short duration experiments, where a paramagnetic current was observed (Hugrass *et al.* 1980). The reason for the difference is not known.

Fig. 14 shows the measured penetration of the applied rotating field into the plasma, without and with the presence of a toroidal field. The measured RF power inputs for the two cases are shown in Fig. 15.

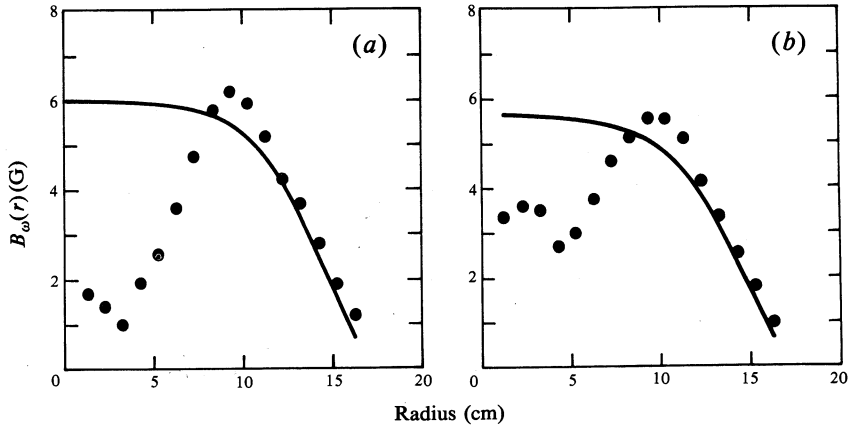


Fig. 14. Penetration of the RF rotating field into the plasma both (a) without and (b) with an applied toroidal magnetic field. The solid curves represent the distribution of the field with no plasma.

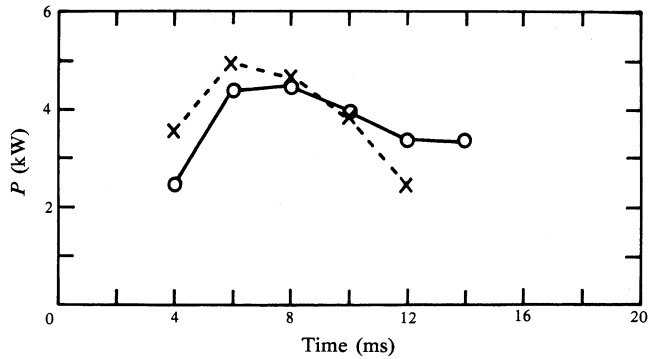


Fig. 15. Estimates of the RF power input into the plasma, both with (dashed curve) and without (solid curve) the toroidal field.

All the above results have been found to be unaffected by a reversal in the direction of the applied toroidal field.

The most important point to note is that a compact torus configuration with an embedded toroidal magnetic field has been maintained in an apparently macroscopically stable manner for at least 6 ms.

The improved penetration of the rotating field when the toroidal field is present is clearly seen in Fig. 14. It is tempting to speculate that the presence of the toroidal field improves the energy confinement, allows the plasma to get hotter, decreases the electron-ion collision frequency, improves the penetration of the rotating field (Fig. 14), decreases the total ohmic dissipation associated with both the toroidal and poloidal currents, and enables the configuration to be maintained at a lower level of RF input power (see Fig. 15 where the input power decreases towards the end of the discharge with the toroidal field present). The reason for the abrupt termination of the configuration with toroidal field has not been investigated.

4. Conclusions

These results confirm that the same general features which were observed in the earlier high power, short duration rotamak discharges are also present in these long duration discharges; namely, that a compact torus configuration is readily generated and maintained, that, provided adequate RF input power is available, the amount of driven toroidal plasma current is dependent on the amplitude of the externally applied equilibrium field, and that the characteristics of the discharge are highly reproducible. Most importantly, the results clearly demonstrate that a compact torus configuration can be maintained for at least 10 ms (limited only by the present duration of the rotating magnetic field) which is equivalent to over 100 Alfvén transit times across the minor diameter. There is no evidence of any gross instabilities. Indeed, the configuration appears extremely robust and shows no tendency to disrupt even when it is subjected to large amplitude, forced oscillations. The reason for this observed stability is not understood at this stage.

Acknowledgments

This work was supported by the Australian Atomic Energy Commission, the National Energy Research, Development and Demonstration Council of Australia, the Australian Institute of Nuclear Science and Engineering, the Australian Research Grants Scheme and the Flinders University Research Budget. One of us (J.E.W.) held an AINSE Studentship while another (M.D.E.T.) held a Commonwealth Post-graduate Research Award during the course of this work.

References

- Blevin, H. A., and Thonemann, P. C. (1962). *Nucl. Fusion Suppl.* Part I, p. 55.
- Durance, G., Jessup, B. L., Jones, I. R., and Tendys, J. (1982). *Phys. Rev. Lett.* **48**, 1252.
- Durance, G., and Jones, I. R. (1986). *Phys. Fluids* **29**, 1196.
- Hugrass, W. N., Jones, I. R., McKenna, K. F., Phillips, M. G. R., Storer, R. G., and Tucek, H. (1980). *Phys. Rev. Lett.* **44**, 1676.
- Hugrass, W. N., Jones, I. R., and Phillips, M. G. R. (1981). *J. Plasma Phys.* **26**, 465.
- Hugrass, W. N., and Kirolous, H. A. (1984). *Aust. J. Phys.* **37**, 521.
- Jones, I. R. (1979). The rotamak concept. Flinders Univ. Rep. No. FUPH-R-151.
- Jones, I. R., and Hugrass, W. N. (1981). *J. Plasma Phys.* **26**, 441.